VOLUMETRIC 3-COMPONENT VELOCIMETRY MEASUREMENTS OF THE FLOW FIELD ON THE REAR WINDOW OF A GENERIC CAR MODEL

by

Nabil TOUNSI [a,b]***, Gregoire FOURRIE*** [a]***, Hamid OUALLI*** [b]***, Laurent KEIRSBULCK*** [a*]***, Samir HANCHI*** [b]***, and Larbi LABRAGA*** [a]

[a] Universite Lille Nord de France, Lille, France; UVHC, TEMPO, Valenciennes, France
[b] LMDF Ecole Militaire Polytechnique, Bordj-el-Bahri, Algiers, Algeria

Short paper
DOI: 10.2298/TSCI 111220036T

Volumetric 3-component velocimetry measurements are carried out in the flow field around the rear window of a generic car model, the so-called Ahmed body. This particular flow field is known to be highly unsteady, 3-D and characterized by strong vortices. The volumetric velocity measurements from the present experiments provide the most comprehensive data for this flow field to date. The present study focuses on the wake flow modifications which result from using a simple flow control device, such as the one recently employed by Fourrié et al. The mean data clearly show the structure of this complex flow and confirm the drag reduction mechanism suggested by Fourrié et al. The results show that strengthening the separated flow leads to weakening the longitudinal vortices and vice versa. The present paper shows that the volumetric 3-component velocimetry technique is a powerful tool used for a better understanding of a 3-D unsteady complex flow such as developing around a bluff-body.

Key words: *volumetric 3-component velocimetry, Ahmed body, aerodynamics, wake flow*

Introduction

The environmental objectives of most transport policies require the development of new road transport strategies in order to improve the energy efficiency of vehicles [1, 2]. The development of sustainable drag reduction devices could be one of the most efficient approaches to reduce both automotive vehicle energy consumption and pollutant emissions. There is ongoing research about how to reduce greenhouse gas emissions via drag reduction. Up to 80% of the aerodynamic drag arises from the low pressure field within the vehicle wake, 30% of which is generated from the flow separation occurring on the rear part of the vehicle. As a consequence, separation control strategies appear to be particularly relevant to reduce both vehicle consumption and emissions.

* Corresponding author; e-mail: laurent.keirsbulck@univ-valenciennes.fr

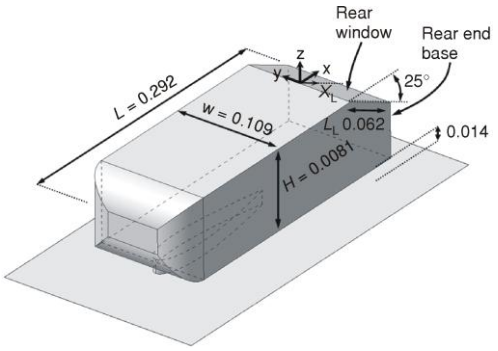

Figure 1. Geometry of the Ahmed model) used in the present study (dimensions in m)

The Ahmed car model is a simplified geometry defined by Ahmed *et al*. [3] (see fig. 1) and commonly used in the vehicle aerodynamics research community. Ahmed *et al*. [3] originally studied the influence of the rear window inclination for cars with a car boot integrated to the main body of the vehicle and topped by a slanted surface, the rear window. The 3-D flow around the Ahmed body is particularly complex above the rear window: two counter-rotating cone-like trailing vortices arise on both lateral edges of the window and interact with the separated bubble developing from the end edge of the roof [4].

In recent years, various flow control strategies have been investigated for this kind of geometry, and in particular for the 25°-inclined rear window Ahmed model (*e. g.* [5-7]). Fourrie *et al*. [8] recently highlighted the effect of a deflector (fixed at the roof end, on the upper edge of the rear window) on both the separated zone and the longitudinal vortices. When the deflection was sufficient, they observed a sudden drag reduction of about 9%, indicating a strong modification in the flow behavior. In that case, they suggested a disturbance of the longitudinal vortex development due to the enlargement of the separated flow region above the window. A quite similar mechanism was suggested by Aider *et al*. [6] for a close geometry. At the same time, Fourrie *et al*. observed the merging of the separated region and the upper recirculation structure at the rear end base.

The aim of the present work is to improve the understanding of the flow topology modification observed in [8] using Volumetric 3-component Velocimetry (V3V) measurements, with emphasis on the region located above the rear window.

Experimental set-up

Two different experimental configurations are considered in our study: a water tunnel with a 0.28:1-scale model and the same wind tunnel and model as in [8].

Water tunnel experiments

Most of the experimental work presented in the present paper was performed in a water tunnel at the TEMPO laboratory of the University of Valenciennes. The test section is 1.2 m long with a 0.3 m × 0.3 m^2 square cross-section. The upstream velocity is 3 m/s and the turbulence intensity is less than 1.5% in empty test section. There are important topology differences between the flows for a reference Ahmed body and for the same body with a deflector inclined at optimum angle. Our work aims at better describing these changes, hence our choice of two models, one for each configuration.

The two models are obtained via stereolithography at a 0.28:1-scale (the reference case is show in fig. 1), which corresponds to a Reynolds number based on the model height of $2.4 \cdot 10^5$. The two models stand on a NACA0018 airfoil profile. The origin of the co-ordinates

is set at the medium point of the upper edge of the rear window and the co-ordinate directions are shown in fig. 1.

All the measurements in the water tunnel configuration are carried out using the TSI's V3V technique. This method is based on the work of Willert *et al*. [9] and of Pereira *et al*. [10]. The main principle is quite similar to that of the standard particle image velocimeter (PIV), where image pairs acquired with a known time delay allow the characterization of particle displacements within an illuminated space in the flow. In the V3V method, three cameras at various small angles focus on a light cone volume. The cameras give three images allowing a volumetric mapping of the particles positions. A preliminary calibration is required and performed by moving a planar target in different measurement planes. The cameras depth of field is checked to be sufficient. Once the seeding particles are identified in each camera image, the same particle observed from the three images is used to define a "triplet". In fact, this triplet forms a triangle in the main resulting focal plane, its size depending on the depth position of the particle (its z co-ordinate). The mean position of the triplet (the center of the triangle) gives the position (x and y co-ordinates) of the particle in the plane located at the depth position determined previously. Then, the velocity vector can be extracted using the tracking method defined by Pereira *et al*. [11]. Unlike the standard PIV, the vector extraction is not performed on a specific grid which makes it necessary to interpolate the resulting vectors on a regular grid.

A schematic view of the system configuration is depicted in fig. 2. The light cone is provided by a double-pulsed Nd-YAG laser operating at 532 nm, with 200 mJ for each pulse and a 7.25 Hz frequency. The flow seeding is performed using polyamide particles with a mean diameter of 50 μm. Three cameras, each with 2,048 × 2,048 pixels^2 charge-coupled device (CCD) sensors, are used. The measurement volume, which is 120 mm × 60 mm × 100 mm, is focused above the rear window of the model. The data processing is performed with the TSI's INSIGHT V3V software.

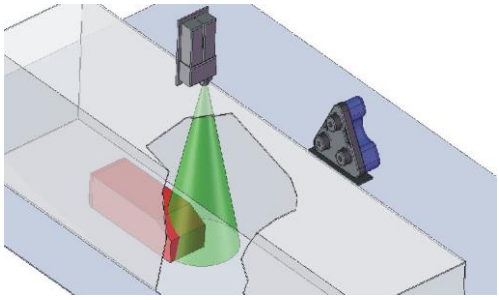

Figure 2. The water tunnel configuration with TSI's V3V system

Wind tunnel experiments

The study involves a spectral analysis from data obtained via hot wire anemometry measurements performed in the wake of the model for the wind tunnel configuration presented previously [8]. The Ahmed body used here is at the scale defined by Ahmed *et al*. [3] (the model is thus 1.044 m long, 0.389 m wide and 0.288 m high). The closed-circuit subsonic wind tunnel has a 10 m long test section with a 2 m × 2 m square cross-section. The turbulence intensity is about 0.5% in empty test section, and the upstream velocity is 16 m/s.

The hot-wire anemometry measurements are performed along two vertical lines behind the model in the middle plane $y = 0$ and at the window height, one very close to the rear end base ($x/L = 0.2$) and the other one farther in the wake ($x/L = 0.4$). Only the spectra at the window lower edge height are presented as they show the most relevant results. Measurements have also been performed along a vertical line outside the middle plane ($y/W =$

= 0.375) but did not provide a relevant spectral behavior. The hot-wire probe used for the measurements is a single-component one and only longitudinal velocity is considered. The probe is made of a 1.25 mm long, 5 μm diameter platinum-plated tungsten wire. A 5th order polynomial approximation is used for velocity calibration. The sampling frequency is 1 kHz and 300,000 samples are considered for each measurement.

The longitudinal vorticity field within a transverse plane behind the model (x/L = = 0.4) is also presented. These results are obtained in wind tunnel using stereoscopic particle image velocimetry (SPIV) measurements.

Results and discussions

Flow topology investigation above the rear window using the V3V technique

As mentioned in [8], in the case of a deflector inclined with an optimum angle, the widening of the separated flow on the upper edge of the window induces the weakening of the longitudinal vortices. Figure 3 shows the loss in coherence of one of these vortices as seen from the longitudinal vorticity field in the wake of the model. This being a view of the aerodynamic field within a plane, no evidence is given of the breaking down of the longitudinal vortex. Moreover, in [8], the SPIV measurements (and standard PIV measurements) did not allow the authors to get an accurate description of the flow topology.

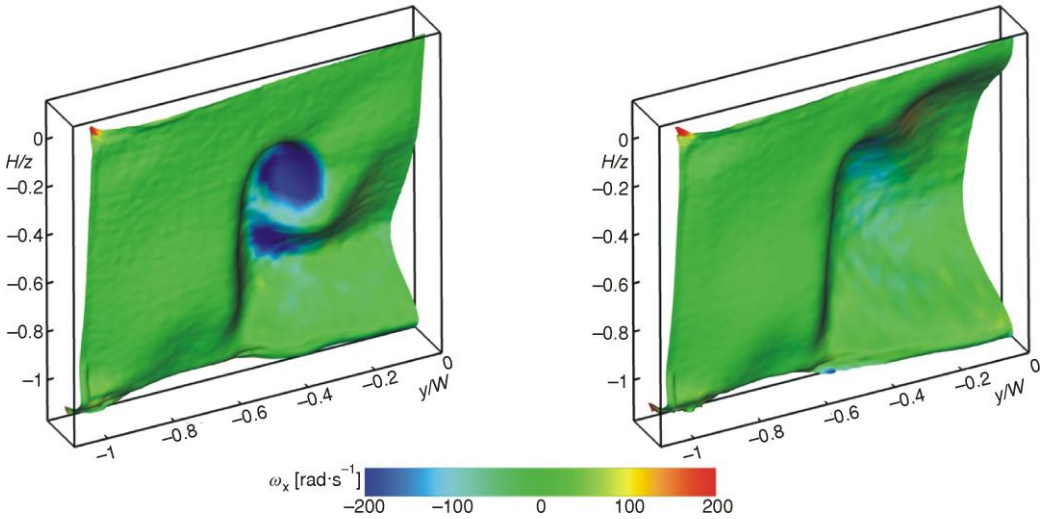

Figure 3. Longitudinal vorticity field in a transverse plane behind the Ahmed model (x/L = 0.4) from SPIV measurements, without (left) and with control device (right). The depth of this vorticity field corresponds to the longitudinal velocity component (color image see on our web site)

Since the V3V technique gives access to the 3-D aerodynamic field, a much better description of the influence of the device on the longitudinal structure development can be achieved. Figure 4 represents iso-vorticity contours (longitudinal and non-longitudinal) above the rear window. The vorticity contours highlight two different kinds of vortex structures. In the reference case, the longitudinal structure is observable, with its core emphasized by the

higher vorticity contour levels. It is now clear from the V3V measurements that the control device leads to the breaking down of the longitudinal vortices. Indeed, even for lower longitudinal vorticity contour values, there is no coherent structure corresponding to the longitudinal vortex. The non-longitudinal vorticity iso-contour highlights the separated flow region above the rear window. This region corresponds to the recirculation bubble in the reference case and to a bulk separation occupying the entire flow volume above the rear window in the case with the control device. This strong separation over the window disturbs the development of the longitudinal vortices and leads to their breakdown.

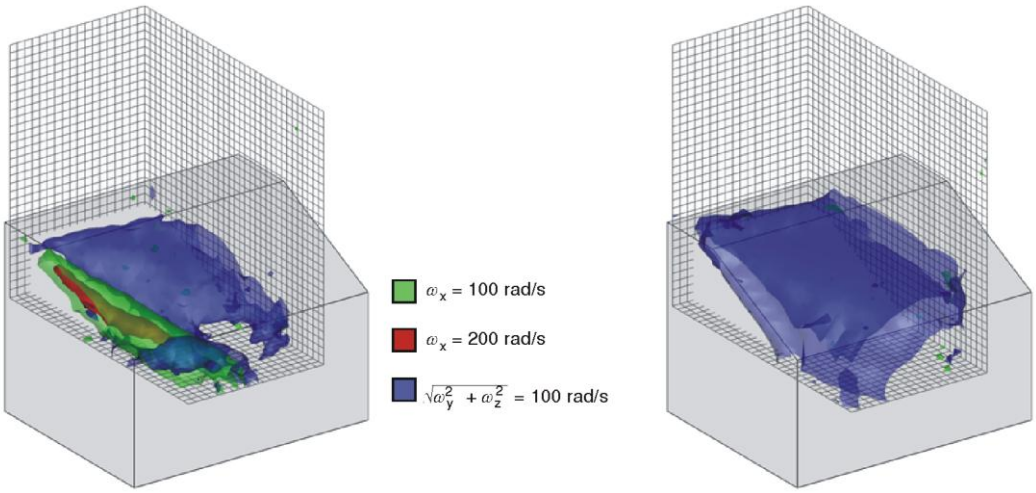

Figure 4. Longitudinal and non-longitudinal vorticity iso-contours, without (left) and with control device (right) (color image see on our web site)

Stream traces (figs. 5 and 6) clearly illustrate the strong flow topology differences between the two considered cases. The reference case (fig. 5) shows a standard behavior, with the rolling up of the stream traces indicating the development of the longitudinal vortex against the separated bubble. In the controlled case (fig. 6), the flow topology is dominated by the bulk separation. The recirculation structure above the window was observed by Fourrie *et al.* [8] to merge with the upper rear end base recirculation. The recirculation core region shows a rolling up from the lateral side of the structure to the inside, in the downward direction. Then, the flow comes back from the rear end base and the stream traces pass over the window and impact it. This structure is highly 3-D with a main distribution inside the vortex structure from the spanwise direction. This complex flow topology could obviously not be determined from the previous PIV

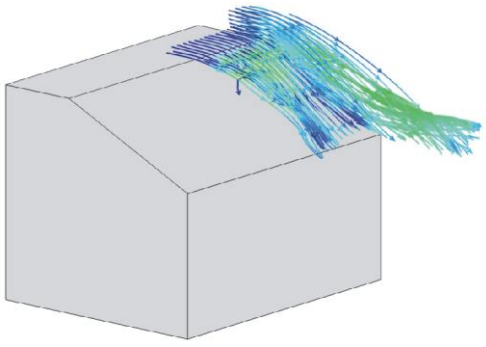

Figure 5. Stream traces above the rear window of the reference case; streamlines colored by the vorticity magnitude

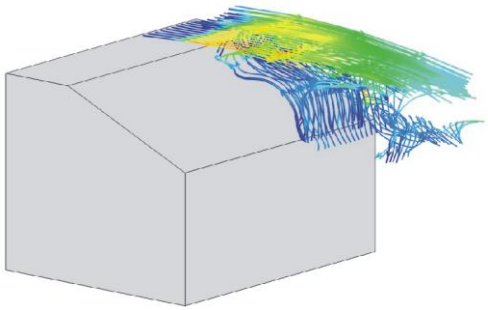

Figure 6. Stream traces above the rear window of the controlled case; streamlines colored by the vorticity magnitude

measurements, even by using SPIV measurements. Although the longitudinal vortices developing in the Ahmed body wake are known to be particularly intense, the controlled flow shows even higher vorticity magnitude levels (fig. 5 and 6).

Influence of the control device on the unsteadinesses around the rear window

Few authors have considered the unsteady phenomena that exist around the Ahmed model (without flow control device). Two main frequencies have been noticed in the literature around the rear part of this geometry. In the present work, the frequency is normalized by the square root of the frontal area of the body resulting in the Strouhal number $St_A = f(HW)^{1/2}/U_0$, where f is the frequency and U_0 the upstream velocity.

The most frequently observed frequency, $St_A \approx 0.5$, corresponds to the von Karman-like vortex shedding from the rear end base (*e. g.* Sims-Williams *et al.* [12] or Minguez *et al.* [13]). A second value observed by Thacker [14], $St_A \approx 0.2$, corresponds to the low frequency flapping of the separated bubble, a phenomenon which is similar to the one existing in the recirculation structure on a thick plate leading edge (see Kiya *et al.* [15]) or downstream of a backward facing step (see *e. g.* Hudy *et al.* [16]). As observed in some studies, this flapping can be accompanied by a vortex shedding.

Hot-wire anemometry measurements are performed in the model near wake in the wind tunnel. The power spectral density from the corresponding velocity signals are presented in fig. 7. Close to the window lower edge, a weak peak around $St_A = 0.23$ is observed in the uncontrolled case. This can be identified as the low frequency related to the separated bubble. This peak does not appear in the controlled case, since the separated bubble no longer exists. Farther in the wake, peaks are observed in both the reference and the controlled cases at St_A = = 0.47 and 0.45, respectively. These are typical for the von Karman-like vortex shedding from

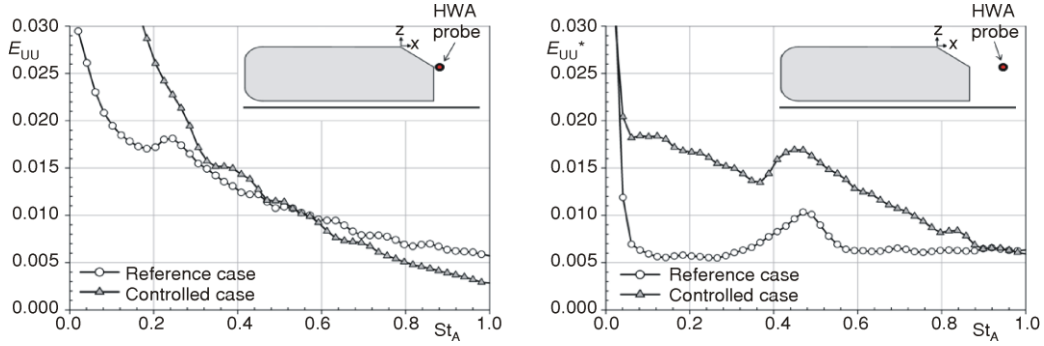

Figure 7. Power spectral densities in two different points downstream the model, at x/L = 0.2 (left) and 0.4 (right); (E_{uu} is the energy spectrum of the streamwise velocity component, normalized by its variance)

the vertical base. Even if the size of the upper structure involved in this shedding mechanism is strongly increased, the shedding frequency is not much affected. Thus, the main unsteady modification is the disappearance of the low frequency related to the separated bubble. The von Kármán-like vortex shedding frequency remains nearly constant.

Concluding remarks

V3V measurements have been carried out to improve the understanding of the flow topology modification induced by a deflector located on the upper edge of the rear window as studied previously in Fourrie *et al.* [8]. The V3V technique allows the measurement of the 3-D velocity field above the rear window. A much more complex flow than previously mentioned is observed when the control device is applied. Iso-surfaces of quantities such as the velocity or the vorticity help in visualizing the structures of the flow and identifying the different regions contributing to drag reduction. These results show the competition between the longitudinal vortices and the separated flow over the window: enhancing one of the structures leads to the destruction of the other ones. Part of the influence of the control device on the unsteadinesses occurring above the window was also observed.

The present measurements are the first instantaneous volumetric measurements of the 3-D flow over the rear window of an Ahmed body and show the high potential of the V3V technique to investigate a complex unsteady 3-D flow.

Acknowledgments

The present research work has been supported by Campus International pour la Sécurité et l'Intermodalité des Transports, la Région Nord-Pas-de-Calais, l'Union Européenne, la Direction de la Recherche, Enseignement Supérieur, Santé et Technologies de l'Information et de la Communication et le Centre National de la Recherche Scientifique. The authors gratefully acknowledge the support of these institutions.

The authors thank Jean Stefanini and Martin Hyde from TSI Inc. for their assistance to the measurements using V3V™ Volumetric 3-Component Velocimetry.

References

[1] Manojlović, A. V., *et al.*, Fleet Renewal: an Approach to Achieve Sustainable Road Transport, *Thermal Science*, *15* (2011), 4, pp. 1223-1236
[2] Petersen, M. S., *et al.*, Report on Transport Scenarios with a 20 and 40 year Horizon, Final Report, Funded by DG TREN, Copenhagen, 2009
[3] Ahmed, S. R., Ramm, G., Faltin, G., Some Salient Features of the Time-Averaged Ground Vehicle Wake, SAE paper 840300, 1984
[4] Spohn, A., Gillieron, P., Flow Separations Generated by a Simplified Geometry of an Automotive Vehicle, *Proceedings*, UTAM Symposium on Unsteady Separated Flows, Toulouse, France, 2002
[5] Aider, J. L., Beaudoin, J. F., Wesfreid, J. E., Drag and Lift Reduction of a 3d Bluff-Body Using Active Vortex Generators, *Experiments in Fluids*, *48* (2010), 5, pp. 771-789
[6] Gillieron, P., Kourta, A., Aerodynamic Drag Reduction by Vertical Splitter Plates, *Experiments in Fluids*, *48* (2010), 1, pp.1-16
[7] Brunn, A., *et al.*, Active Drag Control for a Generic Car Model, *Notes on Numerical Fluid Mechanics and Multidisciplinary Design*, *95* (2007), pp. 247-259
[8] Fourrié, G., *et al.*, Bluff-Body Drag Reduction Using a Deflector, *Experiments in Fluids*, *50* (2011), 2, pp. 385-395

[9] Willert, C. E., Gharib, M., Three-Dimensional Particle Imaging with a Single Camera, *Experiments in Fluids*, *12* (1992), 6, pp. 353-358
[10] Pereira, F., *et al.*, Defocusing Digital Particle Image Velocimetry: a 3-Component 3-Dimensional DPIV Measurement Technique. Application to Bubbly Flows, *Experiments in Fluids*, *29* (2000), Suppl., 1, pp. S078-S084
[11] Pereira, F., *et al.*, Two-Frame 3D Particle Tracking, *Measurement Science and Technology*, *17* (2006), 7, pp. 1680-1692
[12] Sims-Williams, D. B., Duncan, B. D, The Ahmed Model Unsteady Wake: Experimental and Computational Analyses, SAE paper 2002-01-1315, 2002
[13] Minguez, M., Pasquetti, R., Serre, E., High-Order Large-Eddy Simulation of Flow over the "Ahmed Body" Car Model, *Physics of Fluids*, *20* (2008), 9, pp. 095101.1-095101.17
[14] Thacker, A., Experimental Contribution to the Steady and Unsteady Anlysis of the Flow Behind a Bluff Body (in French), Ph. D. thesis, Universite d'Orleans, Orleans, France, 2010
[15] Kiya, M., Sasaki, K., Structure of Large-Scale Vortices and Unsteady Reverse Flow in the Reattaching Zone of a Turbulent Separation Bubble, *Journal of Fluid Mechanics*, *154* (1985), pp. 463-491
[16] Hudy, L. M., Naguib, A. M., Humphreys, W. M., Wall-Pressure-Array Measurements Beneath a Separating/Reattaching Flow Region, *Physics of Fluids*, 15 (2003), 3, pp. 706-717

Paper submitted: December 2, 2011
Paper accepted: December 5, 2011